Bioorganic & Medicinal Chemistry Letters 19 (2009) 2780–2784

Contents lists available at ScienceDirect

Bioorganic & Medicinal Chemistry Letters

journal homepage: www.elsevier.com/locate/bmcl

# Discovery of 4-azaindoles as novel inhibitors of c-Met kinase

John Porter [a,*], Simon Lumb [a], Richard J. Franklin [a], Jose M. Gascon-Simorte [a], Mark Calmiano [a], Kelly Le Riche [a], Bénédicte Lallemand [b], Jean Keyaerts [b], Helen Edwards [a], Alison Maloney [a], Jean Delgado [a], Lloyd King [a], Anne Foley [a], Fabien Lecomte [a], James Reuberson [a], Christoph Meier [a], Mark Batchelor [a]

[a] UCB Celltech, 216 Bath Road, Slough SL1 3WE, United Kingdom
[b] UCB Pharma, R&D, Chemistry, Chemin du Foriest, B-1420 Braine-l'Alleud, Belgium

ARTICLE INFO

*Article history:*
Received 10 March 2009
Revised 20 March 2009
Accepted 23 March 2009
Available online 27 March 2009

*Keywords:*
c-Met Kinase inhibitor
Hepatocyte growth factor receptor inhibitor
Kinase inhibitor
Azaindole

ABSTRACT

A series of 4-azaindole inhibitors of c-Met kinase is described. The postulated binding mode was confirmed by an X-ray crystal structure and series optimisation was performed on the basis of this structure. Future directions for series development are discussed.



Members of the receptor tyrosine kinase (RTK) family are attractive targets for cancer therapy as inhibition can disrupt signaling pathways that mediate tumour formation and growth.[1] c-Met kinase is a member of this family that, together with its ligand, hepatocyte growth factor (HGF) or scatter factor (SF), is important for normal mammalian development. However, c-Met has been shown to be deregulated and associated with high tumour grade and poor prognosis in a number of human cancers.[2] c-Met can become activated by a variety of mechanisms, including gene amplification and mutation inducing motility, invasiveness and tumourgenicity into the transformed cells.[3] Activation leads to receptor dimerisation and recruitment of several SH2 domain containing signal transducers that activate a number of pathways including the Raf-Mek-Erk and PI3k-Akt cascades. Targeting the ATP binding site of c-Met is a popular strategy for inhibition of the kinase, with a number of drug candidates reaching the clinical trials phase.[4] We now wish to report our efforts in this area.

Using our knowledge of the ATP-binding site of kinases in general and c-Met in particular, we identified a series of scaffolds that could potentially form either monodentate or bidentate H-bonds with the kinase hinge residues. Consideration of docked models of these scaffolds allowed us to determine appropriate positions for the addition of suitable substituents to interact with key structural or functional features in the kinase. These elaborated scaffolds were then prioritised on the basis of synthetic tractability and novelty. During this process we observed that the 4-azaindole **1** had moderate activity against c-Met in a biochemical assay[5] ($IC_{50}$ 3.5 μM) and decided to study this scaffold further.

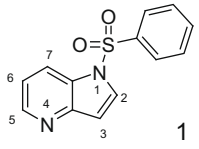


1

The sulphonylated 4-azaindoles were prepared as shown in Scheme 1, by treatment of the commercially available azaindoles with the appropriate sulphonyl chloride. Where functionality was present in the 6-position, this was protected as appropriate prior to the sulfonylation and then elaborated.

Sulphonylated 7-azaindoles were also studied for comparative purposes, their preparation is shown in Scheme 2, starting from the commercially available 7-azaindole. Addition of 2 equivalents

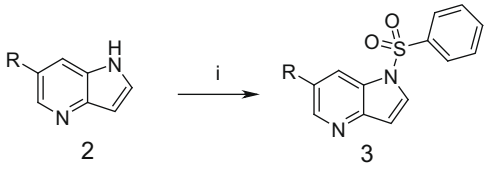


2 3

**Scheme 1.** Preparation of sulphonylated 4-azaindoles. Reagents and conditions: (i) $PhSO_2Cl$, $Et_3N$, THF.

* Corresponding author. Tel.: +44 1753 534655.
*E-mail address:* john.porter@ucb.com (J. Porter).

0960-894X/$ - see front matter © 2009 Elsevier Ltd. All rights reserved.
doi:10.1016/j.bmcl.2009.03.110

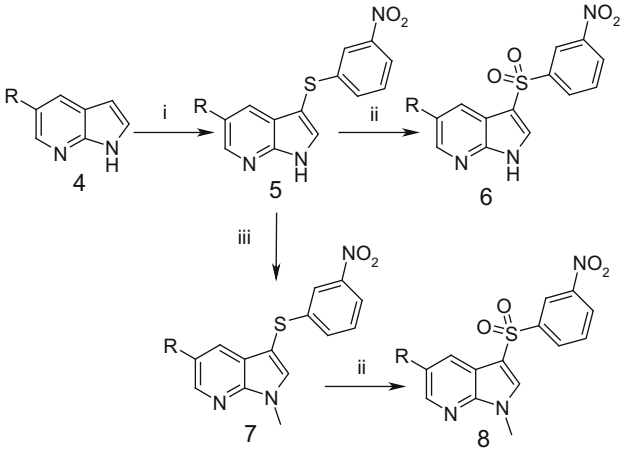

**Scheme 2.** Preparation of sulphonylated 7-azaindoles. Reagents and conditions: (i) NaH, DMF, bis(3-nitrophenyl)disulphide; (ii) mCPBA, $CH_2Cl_2$; (iii) NaH, DMF, MeI.

of base followed by the appropriate disulphide gave selective addition at the 3-position.

The sulphonylated pyrrolopyrazine **12** was prepared as shown in Scheme 3 using a modification of a reported route[6] with a palladium catalysed heteroannulation of the pyrazine **9**, followed by deprotection and sulphonylation. Alkylated 4-azaindoles were prepared as shown in Scheme 4 by deprotonation of the azaindole followed by addition of the appropriate bromides.

Initial efforts aimed at exploring the SAR focused on the phenylsulphonyl group; activities for a representative selection of compounds are shown in Table 1. Substitution in the 3-position generally leads to a loss in potency, however, substitution in the 2-position resulted in an improvement (compare **16** with **17**).

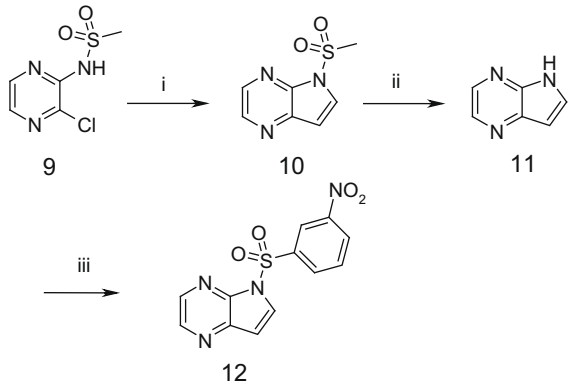

**Scheme 3.** Preparation of pyrrolopyrazines. Reagents and conditions: (i) TMS-acetylene, LiCl, $PdCl_2$(dppf), $Na_2CO_3$, DMF; 100 °C; (ii) $Cs_2CO_3$, THF, MeOH; (iii) 3-nitrophenylsulphonyl chloride, $Et_3N$, THF.

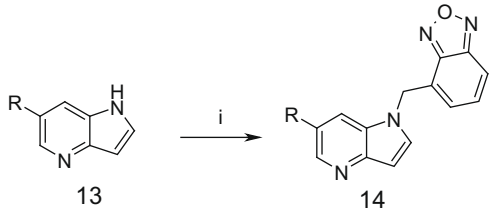

**Scheme 4.** Preparation of non-sulphonylated 4-azaindoles. Reagents and conditions: (i) NaH, DMF, THF, 5-bromomethyl-benz[1,2,5]oxadiazole.

**Table 1**
SAR for 4-azaindoles and pyrrolopyrazines

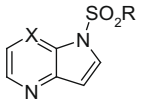

| Compd | R | X | c-Met $IC_{50}$ (nM) |
|---|---|---|---|
| **15** | Phenyl | CH | 3500 |
| **16** | 3-Chlorophenyl | CH | 5670 |
| **17** | 2-Chlorophenyl | CH | 900 |
| **18** | 2,3-Dichlorophenyl | CH | 100 |
| **19** | 2,5-Dichlorophenyl | CH | 2030 |
| **20** | 2,6-Dichlorophenyl | CH | 480 |
| **21** | 3-Nitrophenyl | CH | 70 |
| **22** | 2-Nitrophenyl | CH | 20 |
| **23** | 4-Nitrophenyl | CH | 16% @ 20 μM |
| **24** | 3-Methoxyphenyl | CH | 4600 |
| **25** | 3-Aminophenyl | CH | 4400 |
| **26** | 3-Methylsulphonyl phenyl | CH | 25,200 |
| **12** | 3-Nitrophenyl | N | 1730 |

Interestingly, 2,3-disubstitution, for example, **18**, gives an even greater increase. However, it was with the incorporation of a nitro group, **21** and **22**, that we observed the greatest enhancement in potency, though similar substitution in the 4-position, **23**, abolished activity.

A limited study of the scaffold showed that the introduction of a second nitrogen atom in the pyridine ring (i.e., **12**) reduced potency, presumably because of reduced H-bonding to the hinge residues. Modeling studies had showed that the 3-sulphonylated 7-azaindole would be expected to form a bidentate H-bond with the residues in the hinge region of the kinase with a consequent improvement in potency. This regioisomer would also avoid the potential for the sulphonylaryl group to act as a leaving group. However, the expected improvement in activity was not observed, Table 2. Interestingly, N-methylation of the indole, to give **30**, did not abolish activity suggesting that the pyridine N atom-hinge H-bond was a major contributor to binding potency. As the 7-azaindole scaffold had been used quite extensively in a number of kinase inhibitors,[7] we returned to the 4-azaindole series with the belief that optimisation of the substitution pattern would improve potency.

A systematic study of the 4-azaindole scaffold revealed that the 6-position would be suitable for further potency optimisation studies. It was found that a range of substituents could be accommodated at this position but the amine functionality, especially piperazine groups appeared to be preferred, Table 3. In an attempt to rationalise these observations we solved the X-ray crystal structure of the c-Met-**32** complex, Figure 1.[8] The binding mode was revealed to be as we had predicted with the 4-N atom of the azaindole forming an H-bond to the hinge Met1160, the 2-nitrophenyl ring π-stacking to Tyr1230, the nitro group forming an H-bond to the backbone NH of Asp1222 and the carboxamide group pointing toward solvent. The same conformational change to

**Table 2**
SAR for 7-azaindoles

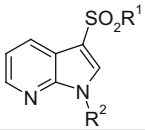

| Compd | $R^1$ | $R^2$ | c-Met $IC_{50}$ (nM) |
|---|---|---|---|
| **27** | Phenyl | H | 1175 |
| **28** | 3-Nitrophenyl | H | 200 |
| **29** | 2-Nitrophenyl | H | 75 |
| **30** | 3-Nitrophenyl | Me | 8100 |

**Table 3**
SAR of 2-nitrophenyl analogues

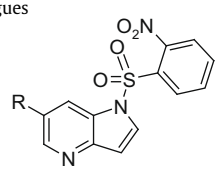

| Compd | R | c-Met $IC_{50}$ (nM) |
|---|---|---|
| **31** | $CO_2H$ | 310 |
| **32** | $CONH_2$ | 82 |
| **33** | 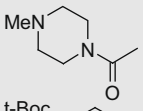 | 300 |
| **34** | 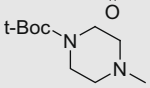 | 20 |
| **35** | 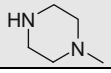 | 20 |

Tyr1230 that we had observed with our quinoxaline inhibitors was also evident.[9]

Attention now turned to stabilising the arylsulphonamide. Results from hepatocyte stability studies and observations during synthesis suggested that the arylsulphonamide was relatively labile, and that this was enhanced by the electron withdrawing properties of the nitro group making the sulphonyl group prone to nucleophilic attack. Attempts to sterically block access to the sulphonyl group by introducing a methyl group at the 2-position of the azaindole gave compounds with a substantial drop in potency. Incorporation of benzofurazan as a nitrophenyl isostere, a modification that had proved successful in our quinoxaline series,[9] gave a compound that was equipotent (compare **36**, Table 4 with **22**, Table 1). A search for other suitable 2-nitrophenyl replacements was conducted by constructing a 76-membered library of sulphonamides prepared by the reaction between the 4-azaindole and readily available sulphonyl chlorides. This library identified the imidazo[2.1.*b*]thiazole group as a potential replacement, based on their potency profile in the biochemical assay, Table 5. Docking suggests that the thiazole ring can π-stack with Tyr1230, the 7-N imidazothiazole atom can H-bond with the backbone N-H of Asp1222, see Figure 1, and the chlorine atom enters a hydrophobic pocket formed by Leu1157, Ala1226 and Leu1140. Combination of the imidazothiazole and a solubilising group at the 6-position gave **46** that had promising activity, Table 5. The imidazothiophene also appeared to stabilise the sulphonamide. For example, whereas **35** had an hepatocyte clearance rate that was too rapid to measure, **45** and **46** had rates of 1.0 and 0.3 $s^{-1}$, respectively.

**Table 4**
SAR of benzofurazan analogues

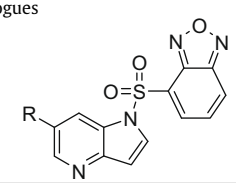

| Compd | R | c-Met $IC_{50}$ (nM) | MKN-45 $IC_{50}$ (nM) | A549 $IC_{50}$ (nM) |
|---|---|---|---|---|
| **36** | H | 22 | nd | nd |
| **37** | 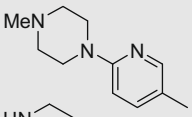 | 15 | 820 | 1310 |
| **38** | 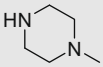 | 23 | nd | nd |
| **39** | 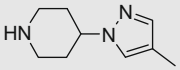 | 9 | 200 | 130 |
| **40** | $NH_2$ | 16 | 1300 | 2200 |
| **41** | 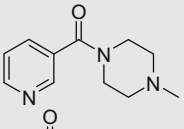 | 11 | 480 | 430 |
| **42** | 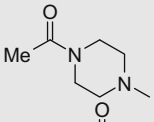 | 12 | 370 | 500 |
| **43** | 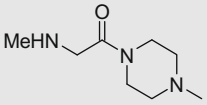 | 14 | 570 | 570 |

nd: no data.

We also investigated potential replacements for the sulphonamide, Table 6. Although the methylene and carbonyl linked analogues were inactive for the nitrophenyl analogues, the methylene linked benzofurazans **55** and **57** did show activity. Interestingly, the two carbon atom linked 2-nitrophenyl analogue **54** also showed promising activity, suggesting that these compounds could form the basis of a new series of c-Met inhibitors.

Compounds with sufficient potency in the biochemical assay were screened in functional cell-based assays using two different cell lines, MKN45 and A549. MKN45 cells are derived from a poorly differentiated gastric adenocarcinoma and have constitutive c-Met activity due to amplification of the c-Met gene locus.[10] These cells represent a ligand-independent cell line in which activation of

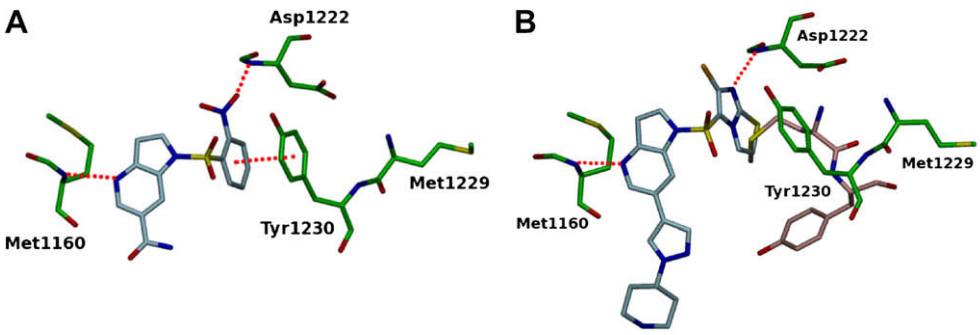


**Figure 1.** (A) X-ray crystal structure of the c-Met (green)/compound **32** (off-white) complex showing key interactions; (B) docking of a model of compound **46** (off-white) with c-Met (green), showing postulated interaction of the imidazothiazole with Asp1222 and Tyr1230. The positions of Met1229-Tyr1230 (from PDB:1ROP) are shown in pink for comparison.

**Table 5**
SAR of imidazo[2.1.*b*]thiazole analogues

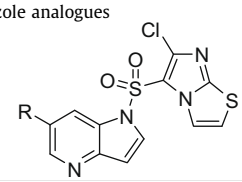

| Compd | R | c-Met $IC_{50}$ (nM) | MKN-45 $IC_{50}$ (nM) | A549 $IC_{50}$ (nM) |
|---|---|---|---|---|
| **44** | H | 35 | | |
| **45** | 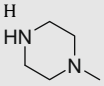 | 24 | 1700 | 1710 |
| **46** | 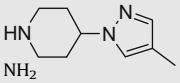 | 9 | 110 | 90 |
| **47** | $NH_2$ | 10 | 490 | 580 |
| **48** | H | 35 | nd | nd |
| **49** | OH | 15 | 3600 | 2810 |
| **50** | 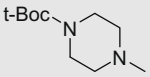 | 27 | 1946 | 110 |
| **51** | 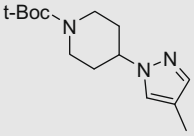 | 19 | 147 | 450 |

nd: no data.

**Table 6**
Non-sulphonylated 4-azaindoles analogues

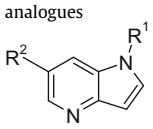

| Compd | $R^1$ | $R^2$ | c-Met $IC_{50}$ (nM) | MKN-45 $IC_{50}$ (nM) | A549 $IC_{50}$ (nM) |
|---|---|---|---|---|---|
| **52** | Benzyl | H | i/a | nd | nd |
| **53** | 2-Nitro benzoyl | H | 12100 | nd | nd |
| **54** | 2-Nitro phenylethyl | H | 250 | nd | nd |
| **55** | 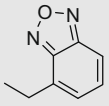 | 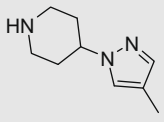 | 19 | 1800 | 1880 |
| **56** | 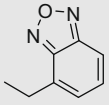 | 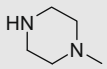 | 1040 | nd | nd |
| **57** | 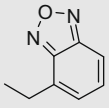 | 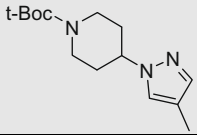 | 33 | 3080 | 3280 |

nd: no data.

c-Met and subsequent downstream signaling are consequences of receptor overexpression. A549 cells are human derived non-small cell lung cancer cells (NSCLC) and in contrast to MKN45 cells, c-Met activation is dependent upon engagement with ligand-independent c-Met phosphorylation[11]). In this assay[12] addition of a solubilising group such as the piperidinyl pyrazole **39** (a group that

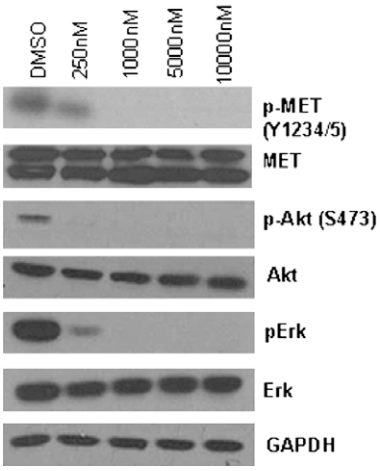


**Figure 2.** Western blot of MKN-45 cells after treatment with compound **39** showing absence of p-Erk and p-Akt.

features in the potent c-Met inhibitor PF-2341066[13]) appeared to enhance potency. Also noteable is the effect of the piperidinyl pyrazole group on the cell-based activity, as shown by comparison of **46** with the piperazine analogue **45**.

In order to exert its cellular functions c-Met signals through multiple downstream signaling pathways, including the mitogen activated protein kinase (ERK1/2) and mediated signaling PI3K/AKT pathways. The Western blot in Figure 2 shows that **39** inhibited c-Met autophosphorylation in MKN-45 cells in a dose dependent manner and, significantly, inhibition of phospho-AKT and phospho-ERK1/2 was also observed.[14] No activity was observed for **39** against AKT and ERK 1/2 in a screen against a panel of 60 kinases.[15]

In conclusion we have identified a novel series of 4-azaindole inhibitors of c-Met kinase. Guided by an X-ray crystal structure we have been able to rationalise the SAR and identified positions where further optimisation would prove profitable.

## References and notes

1. Yasui, H.; Imai, K. *Anti-Cancer Agents Med. Chem.* **2008**, *8*, 470; Alaoui-Jamali, M. A. *Biomed. Pharmacother.* **2006**, *60*, 629; de Jonge, M. J. A.; Verweij, J. *Eur. J. Cancer* **2006**, *42*, 1351.
2. Birchmeier, C.; Birchmeier, W.; Gherardi, E.; van de Woude, G. F. *Nat. Rev. Mol. Cell Biol.* **2003**, *4*, 915.
3. Christensen, J. G.; Burrows, J.; Salgia, R. *Cancer Lett.* **2005**, *225*, 1; Ma, P. C.; Maulik, G.; Christensen, J.; Salgia, R. *Cancer Metastasis Rev.* **2003**, *22*, 309.
4. Cui, J. J. *Exp. Opin. Ther. Patents* **2007**, *17*, 1035; Comoglio, S. G.; Giordano, S.; Trusolino, L. *Nat. Rev. Drug Disc.* **2008**, *7*, 504.
5. $IC_{50}$ values for inhibitors of c-Met were determined using an IMAP Time Resolved Fluorescence Resonance Energy Transfer (TR-FRET) assay. 50 nM 6 His-tagged recombinant human c-Met residues 974-end (Millipore) was incubated in 20 mM Tris, 10 mM $MgCl_2$, 2.5 mM $MnCl_2$, 0.01% Tween 20 and 2 mM DTT with 5 μM ATP and 200 nM 5FAM-KKKSPGEYVNIGFG-NH2 in a total volume of 25 μl for 60 min at ambient temperature. Inhibitors were tested at 10 concentrations starting from 20 μM at a final concentration of 1% DMSO. The reaction was stopped by addition of 50 μl of IMAP Stop solution containing 60%Buffer A:40%Buffer B and a 1 in 400 dilution of beads and Terbium reagent. Plates were read after an overnight incubation at 4 °C on an Analyst HT reader. Reported $IC_{50}$s are from a minimum of 2 experiments ($n = 2$). Data analysis was carried out using a four parameter curve fit. The standard errors of the mean were calculated and expressed as a percentage of the mean $IC_{50}$. The average for this value was 12%.
6. Hopkins, C. R.; Cohen, N. *Tetrahedron Lett.* **2004**, *45*, 8087.
7. For example see: Graczyk, P. P.; Dimopoulos, P.; Khan, A.; Bhatia, G. S.; Farthing, C. N. Patent application WO2008095944.; Ibrahim, P. N.; Artis, D. R.; Bremer, R.; Mamo, S.; Nespi, M.; Zhang, C.; Zhang, J.; Zhu, Y-L.; Tsai, J.; Hirth, K-P.; Bollag, G.; Spevak, W.; Cho, H.; Gillette, S. J.; Wu, G.; Zhu, H.; Shi, S. Patent application WO2007002325.
8. Crystallisation and solution of structure performed by Proteros Biostructures GmbH, Am Klopferspitz 19, D-82152, Martinsried, Germany, www.proteros.com. Crystallographic data for the structure in this paper have been deposited with the PDB (pdb code 2wd1).

9. Porter, J.; Lumb, S.; Lecomte, F.; Reuberson, J.; Foley, A.; Calmiano, M.; Le Riche, K.; Edwards, H.; Delgado, J.; Franklin, R. J.; Gascon-Simorte, J. M.; Maloney, A.; Meier, C.; Batchelor, M. *Bioorg. Med. Chem. Lett.* **2009**, *19*, 397.
10. Nakamura, T.; Matsumoto, K.; Kiritoshi, A.; Tano, Y.; Nakamura, T. *Cancer Res.* **1997**, *57*, 3305.
11. Rege-Cambrin, G.; Scaravaglio, P.; Carozzi, F.; Giordano, S.; Ponzetto, C.; Comoglio, P. M.; Saglio, G. *Cancer Genet. Cytogenet.* **1992**, *64*, 170.
12. All cells were seeded at 20,000 cells/well in a 96-well microplate in RPMI/20% FBS/2 mM glutamine. Compound treatments at 6 dilutions were performed for 1 h at 37 °C followed by immediate 30 min lysis on ice with MSD lysis buffer and frequent vortexing. Lysates were centrifuged at 2500 rpm for 10 min at 4 °C. All washes were performed four times using MSD wash buffer. MSD plate blocking and all other incubations were carried out for 1 h at room temperature with rocking. MSD c-Met (pY1349) 96-well plates were blocked with 3% BSA/MSD wash buffer followed by washing. Twenty-five microlitres of supernatant were added to each well and incubated as previously described, followed by washing. Each well was incubated with 25 μl of detection antibody (anti-total Met)/1% BSA/MSD wash buffer followed by washing. Read buffer (150 μl) was added to each well and the plates were read on a MSD SECTOR™ 6000 Instrument. Background BSA signals were subtracted from pY1349 signal for each well and IC50s were determined using XLfit 4.2 software.
13. Zou, H. Y.; Li, Q.; Lee, J. H.; Arango, M. E.; McDonnell, S. R.; Yamazaki, S.; Koudriakova, T. B.; Alton, G.; Cui, J. J.; Kung, P.-P.; Nambu, M. D.; Los, G.; Bender, S. L.; Mroczkowski, B.; Christensen, J. G. *Cancer Res.* **2007**, *67*, 4408; Cui, J. J.; Botrous, I.; Shen, H.; Tran-Dube, M.; Nambu, M.; Kung, P. P.; Funk, L.; Jia, L.; Meng, J.; Pairish, M.; McTigue, M.; Grodsky, N.; Ryan, K.; Alton, G.; Yamazaki, S.; Zou, H.; Christensen, J.; Mroczkowski, B. *Abstracts of Papers*, 235th ACS National Meeting, New Orleans, LA, United States, April 6–10, 2008, MEDI-177.
14. MKN-45 cells were cultured in RPMI 1640 medium containing 20% serum and pretreated for 1 h at 37 °C with increasing concentrations of compound or DMSO, cells were then lysed in RIPA buffer containing appropriate inhibitors. Western blotting was carried out following standard procedures and probed with the following antibodies: anti-phospho c-Met (Tyr -234/5), anti-c-Met, anti-phospho AKT (Ser 473), anti-AKT, anti-phospho ERK1/2 (Thr 202/Tyr 204), anti ERK1/2 (Cell Signaling Technologies Inc.), following the manufacturer's protocol. Total cellular protein loadings were semi-quantified by probing with anti-GAPDH.
15. **39** was screened against a 60 member kinase panel by Millipore Bioscience Division, Millipore UK Ltd, Gemini Crescent, Dundee Technology Park, Dundee, DD2 1SW, United Kingdom. www.millipore.com. Results were expressed as percentage of activity remaining @ 20 μM: both AKT and ERK1 having 88% activity remaining. This screen did show that **39** had some activity against KDR, Mer, TrkA and Ron (3%, 19%, 18% and 29% activity remaining respectively).